AN EXAMINATION OF PHYSICAL BIASES IN CLIMATE MODELS AND THEIR IMPLICATIONS FOR OCEANIC CARBON UPTAKE

By

Alison Drain, Joellen Russell, and Paul Goodman

A Prepublication Manuscript Submitted to the Faculty of the

DEPARTMENT OF GEOSCIENCES

In Partial Fulfillment of the Requirements

for the Degree of

MASTER OF SCIENCE

In the Graduate College of

THE UNIVERSITY OF ARIZONA

2009

Abstract

The ventilation of Southern Ocean deep water regulates climate through carbon and heat uptake and transport, yet published Southern Ocean transport estimates from data differ widely. We address this uncertainty by analyzing coupled climate model simulations of the late 20th century associated with the Intergovernmental Panel on Climate Change's Fourth Assessment Report (IPCC-AR4) in terms of their volume, heat and "carbon" transport across 30°S, into and out of the Southern Ocean. We quantify these transports in each of the observationally based layers of the water column and compare them to published inverse model analyses of hydrographic data. IPCC-AR4 coupled climate models do not simulate a carbon cycle so we calculate each model's "implied carbon transport" by mapping observed carbon concentrations from the Global Ocean Data Analysis Project (GLODAP) onto model velocity fields. The strength and position of the sub-tropical gyres controls the accuracy and precision of the heat transport, but deep ocean exchange is most important for carbon transport. This study has broad implications for future simulations of the global ocean's response to climate change, highlighting the importance of Southern Ocean physics for the magnitude and direction of global carbon exchange in the future.

1. Introduction

The Southern Ocean is a critical component of the climate system, the global carbon cycle and of patterns of climate change; it alone accounts for roughly 40% of global oceanic uptake of anthropogenic carbon dioxide (CO_2) [*Sabine et al.,* 2004]. The rate of heat and carbon uptake by the Southern Ocean is limited by the rate at which water is exposed to the surface and transported out of the region, but published observation-based and model-based estimates for Southern Ocean water mass transformations differ considerably from one another (see Table 1). The simulated overturning rates disagree: numerical, ocean-only, and global climate models (GCMs) project a range of transformation rates owing to, among other things, different vertical diffusion coefficients and variations in wind stress [*e.g., Hallberg and Gnanadesikan,* 2006; *Gnanadesikan,* 1999; *Russell et al.,* 2006a]. Differences in layer definitions (as in Table 1) complicate water mass transport comparisons between these studies. Even when layer definitions are roughly comparable, as in Ekman and surface layer definitions between the studies in Table 1, the wide range of transport estimates illustrates that uncertainties inherent in each studies' datasets and technique confuse our understanding of Southern Ocean behavior.

Our analysis compares observation-based inverse estimates of volume and heat transport from the Southern Ocean at 30°S with "pseudo-inverse" estimates calculated from the IPCC AR4 model output for the late 20th-century model runs. We find that model errors can vary widely and indiscriminately: one model that has too much water in a certain density range moving too slowly can be nearly indistinguishable from another with too little water moving too fast. Attributing errors in heat transport is even more problematic because errors can be associated with either temperature or velocity variables. We consider these caveats in our analysis.

These modeled circulation differences lead to a wide range of projections for the net oceanic uptake of anthropogenic carbon by the Southern Ocean [*Friedlingstein et al.,* 2006, *Russell et al.,* 2006b]. *Stouffer et al,* [2006] note that the global surface air temperature rise is directly related to the heat uptake by the Southern Ocean, and *Monaghan et al*. [2008] found that GCMs overestimate the warming rate over Antarctica by a factor of 2.5-5. From these studies, we infer that the models underestimate both the heat uptake and the carbon uptake in Southern Ocean. In order to differentiate between the effects of circulation errors (where water at a particular location and depth doesn't move as observations say it should) and water mass errors (a model represents the wrong type of water at a given location and depth), we map the observed carbon concentrations from the Global Ocean Data Analysis Project [GLODAP; *Key et al.,* 2004] onto modeled velocity fields. We can then estimate how much carbon a model would transport if its carbon profile were perfectly simulated. The technique also gives insight into determining whether a given model error is due to problems with the circulation or due to definitions of the water density layers, which are based on tracer data.

Our analysis reveals that more of the model differences and errors are due to circulation errors rather than layer definitions. Our results have broad implications for future simulations of the global ocean's response to climate change, especially for simulations of the carbon cycle. A description of the data against which we compare model output and our methods of calculating layer transports for volume, heat, and implied-carbon are included in section 2. In section 3 we describe the results of our analysis. Our discussion of the implications of our results is in Section 4, and Section 5 details our conclusions.

2. Methods

Inverse analysis methods are standard oceanographic tools for determining transports from hydrographic measurements. But certain assumptions, including water velocities, are necessary to solve the underdetermined set of equations. This leaves open the possibility that more than one solution will be consistent with observations. Since there are no standard criteria for the layer or water mass definitions, published transport estimates from the Southern Ocean vary widely (Table 1). Consider the export of water nominally called Mode and Intermediate water. Each of the studies uses a different set of density ranges, and as a result, exports vary from 2-42 Sv. The advantage of using models is that they produce a known velocity field; from this information we can calculate water budgets and heat and carbon transports in a "pseudo-inverse" fashion.

One of the most recent and self-consistent inverse analyses of the Southern Ocean comes from *Talley* [2008] (T08 hereafter). This study divides the water column into 12 different layers for each of the three oceanic basins (Indian, Pacific, Atlantic) and creates a uniform framework for analyzing the flow into and out of the Southern Ocean at 30°S. We use the layer definitions found in that study (T08, Table 14) with one exception: we do not separate out the Ekman transport from the rest of the surface layer. Instead we assume that all of the Ekman flow is part of the uppermost layer, so our pseudo-inverse calculation, then, uses 11 layers instead of 12. The layer interfaces in this study are at σ_θ = 26.1, 26.4, 26.9, 27.1, and 27.4, σ_2 = 36.8, and σ_4 = 45.80, 45.86, 45.92, and 46.00.

Using these layer definitions, we calculate pseudo-inverse volume, heat, and carbon transports based on output from a subset of the IPCC-AR4 coupled climate models. We use output from each model's the 20th century simulation (20C3M) in this study. All the model

output used in this analysis as well as additional documentation are available from the Program for Climate Model Diagnosis and Intercomparison (PCMDI) at http://www-pcmdi.llnl.gov/.

Our attribution of physical biases requires that we isolate circulation errors from errors associated with any T08 tracer-derived layer definitions. As described in *Bindoff and McDougall* [1994], temperature and salinity observations at fixed depths are affected by variations in isopycnal heights, which can occur in the absence of water mass change. To remove this "heaving" effect, which can mask the true nature of water mass transports, we subdivide each of the layers (excluding the bottom-most layer) into four sublayers as in *Russell et al.* [2006a]. Sublayers detail water velocities and volumes on a smaller scale that can be lost in the averaging across a larger, more coarsely defined density layer. We use this information to determine whether transport errors are associated with heaving or with true physical circulation biases.

For each of our transport calculations, the given model's temperature and salinity fields are re-gridded onto its velocity grid in order to determine in which density layer to group the transport. Global (or basin-wide) integrals are then calculated and the simulated or interpolated value at 30°S is used.

2.1 Volume Transports

We begin by calculating volume transport across the section in each density class by:

$$V = \iint v \, dA \quad (1)$$

where v is the velocity normal to the area (m s^{-1}), and is integrated over a vertical section $dA = dxdz$. A separate integration is done for each density layer.

2.2 Heat Transports

After *Talley* [2003], we compute heat transport in terms of the total temperature carried into a closed region as one way of evaluating model physics. Temperature transport is given by:

$$H = \iint \rho v c_p \theta \, dA \quad (2)$$

where ρ, θ, v, and c_p are in situ density (kg m^{-3}), potential temperature referenced to the surface (°C), velocity normal to the area of the cross-section (m s^{-1}), and specific heat of seawater (we use a constant 4000 J kg^{-1} $°C^{-1}$). Heat transports are given in petawatts (1 PWT = 10^{15} J s^{-1}). The observed values used are from WOA01 [*Conkwright et al*., 2002].

2.3 Carbon Transports

We calculate the models' "implied carbon transports" in an analogous fashion.

$$C = \iint \rho v [TCO_2] \, dA \quad (3)$$

where ρ, v, and $[TCO_2]$ are in situ density (kg m^{-3}), velocity normal to the area of the cross-section (m s^{-1}), and total carbon concentration (μmol/kg) from GLODAP [*Key et al*., 2004]. Units of transport are converted to petagrams (1 Pg = 10^{15}g) of carbon per year (Pg/yr) by multiplying the above integral by the molecular weight of carbon (12 g mol^{-1} = 1.2e^7 g μmol^{-1}) and the number of seconds in a year. Averaging the GLODAP TCO_2 in each of the T08 layers in

the WOA01 and multiplying this average by the T08 transport estimate gives observed carbon transport. We calculate the total transport across 30°S to be ~0.6 Pg/yr northward which agrees well with the *Gurney et al.* [2002] estimate of 0.5±0.3 Pg/yr from atmospheric transport models.

Figure 1 demonstrates the usefulness of the technique: carbon transports calculated by multiplying each model's velocities with the observed GLODAP data (bottom) are nearly identical to those calculated from the modeled carbon field (top, OCMIP2 abiotic simulation, data courtesy of R. Slater) within the section. Using GLODAP data instead of model biogeochemistry removes one degree of uncertainty that the different models' components introduce, allowing us to focus more clearly on biases in model physics.

Inverse volume transport calculations for the GFDL-CM2.1 simulation are shown in Figure 2, with T08 inverse estimates superimposed in black outline. The finer, subdivided set of inverse calculations demonstrates that some mismatches in coarse-layer inverse transport estimates can be explained by heaving associated with small differences in the isopycnal layer definitions, as is the case for surface transports and for the Antarctic Intermediate Water layer (AAIW; $26.4\sigma_0<\sigma<27.1\sigma_0$) for the total section at 30°S. To determine if errors are associated not with the model itself but with the T08 layer definitions, we show both coarse and fine transports in the basin intercomparison (Figure 2) and in the model intercomparison (Figure 3).

The Atlantic section agrees well with T08 observations; this model converts a small extra amount of upper water ($\sigma_0<26.4$) into North Atlantic Deep Water (NADW). The modeled overestimate of NADW ($\sigma_0=27.1<\sigma<\sigma_4=45.8$) import to the Southern Ocean counterbalances a lack of deep water transport from the Pacific Ocean southward; summing the three basins partially corrects estimates of water transports in the NADW density class. On the other hand, errors in the model's Indian Ocean intermediate and mode layers increase the error in these

layers when all three basins are summed. Indian Ocean surface transports do stand up well against Talley surface transports; errors in the total surface transport are related to overestimates of northward surface transport in the Atlantic and Pacific basins. Summing model transports within each layer of each basin, then, has the potential to introduce more or less agreement with Talley estimates than any of its basins alone. Since this study focuses on the Southern Ocean as a whole, inter-basin differences in the other models will not be discussed here, but this caveat should be considered when evaluating model results.

3. Results

The amount of water "ventilated" or exposed to the atmosphere in the Southern Ocean depends on two opposing factors: the strength of the wind-driven divergence and the strength of the underlying stratification [*Matear et al.,* 2008]. Ventilating intermediate and mode waters is critical for ocean-atmosphere heat and carbon exchange: more ventilation of these waters results in more oceanic uptake of heat and carbon. An appropriately ventilated model ocean, then, is essential to properly simulate exchange with the atmosphere and heat and carbon transport in the global ocean.

3.1 Volume Transport

All of the models simulate a southward transport in the uppermost fine surface layer (σ_0<24.9) and most of the models (with the exception of CSIRO-Mk3.5 and UKMO-HadCM3) have a net southward transport in the surface layer (σ_0<26.1). With the exception of IPSL, however, all of the models have a net northward flow in the lower thermocline (26.1<σ_0<26.4) counter to the southward transport in this layer in T08.

Also, all of the models underestimate bottom water (σ_4>45.86) transport (with the exception of MIROC (hires), which simulates its bottom water well in the (45.92<σ_4<46.0) density class). Problems with bottom water export cannot be explained by heaving, since many of the models also underestimate NADW (27.1σ_0<σ<45.86σ_4) export to the Southern Ocean. GISS-AOM and IPSL, for example, lack deep and bottom water almost entirely, but they also grossly underestimate NADW transport. Since most of the models underestimate both deep and bottom water transport, the errors in many models' intermediate layers will influence Southern Ocean transports more than they should; this will change how the models ventilate, leading to errors in their carbon transports.

3.2 Heat Transport

Heat and carbon transports for each model scatter around T08 inverse estimates in Figure 4. All models simulate net heat transport to the Southern Ocean, in agreement with observations. Because it can readily exchange energy with the atmosphere, the surface ocean transports the most heat of any layer in the column, and all of the models have this transport into the Southern Ocean. *Russell et al.* [2006a, Fig. 3] showed that most of the models still had westerly flow at this latitude whereas NCEP places this latitude in the tropical easterlies and also that nearly all of the models were colder than observed at 30°S (their Fig. 4). Models with the most vigorous southward surface transports include CCCMA(T47), CCCMA(T63), MRI, IPSL, and MIROC (hires); these models also import the most heat into the Southern Ocean, with the MIROC (hires) model overestimating transport by roughly 0.2PW. In general, *Russell et al.* [2006a] characterized these models as having too strong winds, too far equatorward, leading to extra-vigorous sub-tropical gyres. The GISS-AOM model, in spite of its large southward surface

transports, overestimates its northward transports in the $27.1<\sigma_0<27.4$ density classes, damping its total heat uptake.

The CCCMA(T47), CCCMA(T63) MRI, and IAP heat transports most closely resemble those of observations at a net import (on the order of 0.75-0.85PW) to the Southern Ocean; each of these models is within 0.1PW of observed, well within the range of uncertainty of 10-20% given by *Talley* [2003]. However, they all simulate a good representation of heat transport in spite of model errors: all of these models simulate overly warm western boundary currents implying that their currents are too weak, and the IAP model in particular had a very poor representation of transports at nearly every layer in the column (Figure 3).

3.3 Carbon Transport

Figure 1 shows the layers most critical for global carbon transport at 30°S. The surface flow and NADW are large sources of carbon import to the Southern Ocean and there is substantial export in the bottom water layers and in the intermediate waters. Unlike heat transport, it is necessary to correctly simulate each layer in the water column to correctly simulate carbon transport, since layers throughout the column (and not just the surface layer) are significant sources of carbon import and export.

What we see in Figure 4 is that carbon transports across the models span a wide range of variability. Most models overestimate carbon export, and none of the models seem to get the right export for the right reason, largely because almost all models fail to properly simulate intermediate and mode waters and their deep water import is too weak. The models that simulate transport most closely to observations include CCCMA(T63), CCCMA(T47), IAP, and GFDL-CM2.1. Again, the IAP model performs well in spite of its poor water mass stratification, not

ventilating AAIW vigorously enough and returning some water to the north at depth to account for a small net export of carbon (Figure 3). Similarly, the CCCMA simulations appear to reasonably representation ventilation, though these models, too, underestimate both the northward transport of carbon by bottom waters and the southward transport by deep waters.

The CSIRO models and MIROC(hires) have vigorous (although less than observed) bottom water and too much northward surface/intermediate water transport leading to their large net carbon transports. IPSL, on the other hand has a large northward transport due to the absence of southward flowing deep water. The only model with a strong net import into the Southern Ocean is GISS-AOM due to its excessively southward surface flow and non-existent bottom water flow.

4. Discussion

Our inverse analysis demonstrates that models' Southern Oceans are widely variable. All the models included in this study have substantial transport errors in some or most of the water column. Errors in the simulated flow will have differing effects on the net transport of heat and carbon. Most of the models underestimate deep and bottom water transport, but these shortcomings have little effect on the simulated heat transport, which occurs largely in surface layers. Wide variability in surface simulations, with errors likely associated with both winds and surface fluxes, within the model suite accounts for a roughly 1PW range of heat transport. As *Russell et al.* [2006a] noted, a coupled climate model must strike the right "Goldilocks" balance: gyres that aren't too strong or too weak, combined with surface temperatures that aren't too cold or too warm. In general, our analysis shows that most errors stem from errors in the physics:

models with the lowest net surface volume transports move the least heat, whereas the models with the highest surface volume transports are also those with the highest heat transports.

Carbon transports, on the other hand, are more complicated because substantial carbon transport occurs at almost all isopycnal depths (Figure 1). Proper carbon transport for the "right reasons" would require a good simulation of water mass transports throughout the water column and across the globe. The misrepresentation of carbon transports, the overestimation seen in most models in Figure 4, has important implications for projections of future oceanic carbon behavior, and properly simulating ocean physics is critical to capturing its true transport in the future. Even a cursory look at Figure 3 reveals very large disagreement in water mass transport across the model suite, which ultimately leads to a range in carbon transport on the order of 40Pg/yr. If we are to accept a "good" simulation, such as that from the IAP model, we must be wary of specious agreement with observations: it nearly matches T08 heat and carbon observations in spite of its poor representation of water mass transport. An examination of each model's transports within each of the individual ocean basins will more thoroughly illuminate the sources, magnitude, and importance of each model's water mass errors.

One potentially large source of these physical errors is likely due to the models' mean zonal wind positions, which alter a model's heat and carbon uptake [*Russell et al.,* 2006b]. Errors in wind-driven divergence are difficult to attribute owing to the number of differences between global climate models [*Russell et al.,* 2006a], but it is very likely that the large variability between model winds accounts for some of the physical errors in heat and carbon uptake in the ensemble. Additionally, most models' simulated surface transports have large errors from observed, likely due to problems modeling surface fluxes. Models whose volume transports are

most vigorous throughout the water column are also those that most overestimate carbon export from the Southern Ocean: again, errors are dominated by errors in the physical circulation.

5. Conclusions

We assessed the IPCC-AR4 climate models' simulations of the last 20 years of the 20th century at 30°S, calculating from their output the volume, heat, and carbon transports. Properly capturing the water mass transformation leading to ventilation is necessary to understand oceanic heat and carbon uptake, both at present and in the future. A coupled model's simulation of future climate is largely affected by its ability to simulate Southern Ocean behavior.

We expect that these differences in these models' Southern Ocean late 20th-century climates and their carbon uptake will be augmented as these models project ocean behavior and atmospheric carbon into the year 2100 and beyond. Understanding the sources of these errors is crucial if we are to improve our understanding of ocean carbon behavior in the future. We have shown that there is no easy road to the correct simulation of the Southern Ocean carbon cycle: models must correctly simulate all of the oceans water masses if they are to reliably simulate the anthropogenic perturbations to the global carbon cycle.

6. Acknowledgements

The authors thank Jorge Sarmiento for many helpful discussions. The authors also thank Julie Cole for reviewing earlier versions of this paper. Financial support was from the National Oceanic and Atmospheric Administration under grant number XXXXXX.

References

Dickson, A.G., and C. Goyet, Eds. (1994), *Handbook of Methods for the Analysis of the Various Parameters of the Carbon Dioxide System in Sea Water.* Version 2, ONRL/CDIAC-74, Department of Energy. [Available online at http://132.239.122.17/co2qc/handbook.html.]

Gnanadesikan, A. (1999), A simple predictive model for the structure of the oceanic pycncline, *Science,* **283**, 2077-2079.

Gnanadesikan, A., J.P. Dunne, R.M. Key, K. Matsumoto, J.L. Sarmiento, R.D. Slater, and P.S. Swathi (2004) Oceanic ventilation and biogeochemical cycling: Understanding the physical mechanisms that produce realistic distributions of tracers and productivity, *Global Biogeochem. Cycles*, **18**, GB4010, doi:10.1029/2003GB002097.

Gurney, K.R. et al. (2002), Towards robust regional estimates of CO2 sources and sinks using atmospheric transport models, *Nature*, **415**, 626-630.

Hallberg, R. and A. Gnanadesikan (2006), The role of Eddies in determining the structure and response of the wind-driven Southern Hemisphere overturning: results from the Modeling Eddies in the Southern Ocean (MESO) project, *J. Phys. Oceanogr.,* **36,** 2232-2252.

Key, R.M. et al. (2004), A global ocean carbon climatology: Results from Global Data Analysis Project (GLODAP), *Global Biogeochem. Cycles,* **18,** GB4031, doi:10.1029/2004GB002247.

MacDonald, A. (1998), The global ocean circulation: a hydrographic estimate and regional analysis, *Progress in Oceanography,* **41,** 281-382.

Mataer, R.J. and A. Lenton (2008), Impact of historical climate change on the Southern Ocean carbon cycle, *J. Climate*, **21,** 5820-5834.

Mikaloff Fletcher, S.E. et al., (2006), Inverse estimates of anthropogenic CO2 uptake, transport, and storage by the ocean. *Global Biogeochem. Cycles,* **20***,* GB2002, doi:10.1029/2005GB002530.

Monaghan, A. J., D. H. Bromwich, W. Chapman, and J. C. Comiso (2008), Recent variability and trends of Antarctic near-surface temperature*, J. Geophys. Res*., **113**, D04105, doi:10.1029/2007JD009094.

Randall, D.A., R.A. Wood, and coauthors, 2007: Climate Models and Their Evaluation. In: *Climate Change 2007: The Physical Science Basis. Contribution of Working Group I to the Fourth Assessment Report of the Intergovernmental Panel on Climate Change* [Solomon, S., D. Qin, M. Manning, Z. Chen, M. Marquis, K.B. Averyt, M. Tignor and H.L. Miller (eds.)]. Cambridge University Press, Cambridge, United Kingdom and New York, NY, USA.

Russell, J.L., R.J. Stouffer, & K.W. Dixon (2006a), Intercomparison of the Southern Ocean Circulations in the IPCC Coupled Model Control Simulations, *J. Climate,* **19(18)**, 4560-4575.

Russell, J.L., K.W. Dixon, A. Gnanadesikan, R.J. Stouffer, & J.R. Toggweiler (2006b), The Southern Hemisphere Westerlies in a Warming World: Propping Open the Door to the Deep Ocean. *J. Climate,* **19(24)**, 6382-6390.

Sabine, C.L. et al. (2004), The oceanic sink for anthropogenic CO_2, *Science,* **305**, 367-371.

Sarmiento, J.L., T.M.C. Hughes, R.J. Stouffer, and S. Manabe (1998), Simulated response of the ocean carbon cycle to anthropogenic climate warming, *Nature*, **393**, 245-249.

Sloyan, B.M., and S.R. Rintoul (2001), The Southern Ocean limb of the global deep overturning circulation, *J. Phys. Oceanogr.,* **31,** 143-173.

Talley, L.D. (2003), Shallow, intermediate and deep overturning components of the global heat budget, *J. Phys. Oceanogr,* **33**, 530-560.

Talley, L.D., (2008), Freshwater transport estimates and the global overturning circulation: Shallow, deep, and throughflow components, *Progress in Oceanography,* **78**, 257-303.

Watson, A.J. and J.C. Orr, (2003), Carbon dioxide fluxes in the global ocean. In: Ocean Biogeochemistry, ed. M.J.R. Fasham, Springer-Verlag, Publishers, New York, pp.123-143.

Table 1: Comparison of Published Southern Ocean Transport Estimates

	Hallberg & Gnanadesikan (2006)		Talley (2003)—Reid result		Talley (2008)		Sloyan & Rintoul (2001): 30°-40°S		Gnanadesikan et al. (2004)	
	Definition	Amount In/Out	Definition	Amount In/Out	Definition	Amount In/Out	Definition	Amount In/Out	Definition	Amount In/Out
Ekman & Surface	$\sigma < 36.9\sigma_2$	26 Sv in	Above $27\sigma_0$	9 Sv in	Ekman-surface-to $26.1\sigma_0$	9.2 in	Surface to $\gamma^n=26.0$	4.19 Sv out	Surface to $\sigma_0=26.4$	3.7 in
Mode & AAIW	$33.4\sigma_2$ -$36.1\sigma_2$	42 Sv out	$26.5\sigma_0$ -$27.3\sigma_0$	8.3 Sv out	$26.9\sigma_0$ -$27.1\sigma_0$	11.9 Sv out	$\gamma^n=26.0$-$\gamma^n=27.4$	2 Sv out	$26.4\sigma_0$-$27.4\sigma_0$	16.3 out
NADW	$36.1\sigma_2$ -$37.0\sigma_2$	39 Sv in	$27.3\sigma_0$-$45.88\sigma_4$	21.1Sv in	27.1 σ_0-$45.86\sigma_4$	29.8 Sv in	$\gamma^n=27.4$ $\gamma^n=28.0$	52 Sv in	$27.4\sigma_0$-$45.6\sigma_4$	30.1 in
BW	$\sigma > 37.0\sigma_2$	23 Sv out	$\sigma > 45.88\sigma_0$	22.1 Sv out	$\sigma >$ 45.86 σ_4	27 Sv out	$\gamma^n > 28.0$	46 Sv out	$\sigma_4 > 45.6$	17.2 out

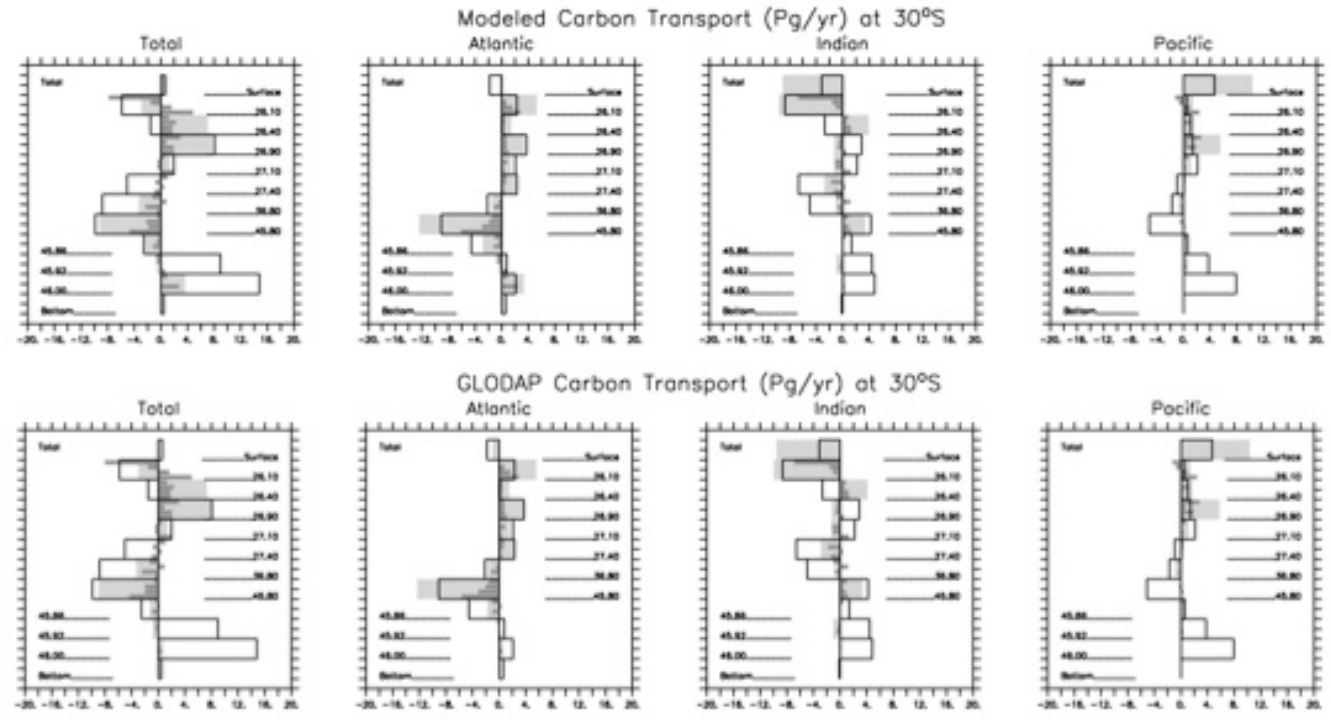

Figure 1.

Comparison of model-computed carbon transports (top row) with carbon transports calculated from the multiplication of model volume transports with GLODAP data (bottom row) [*Key et al.,* 2004]. From left to right are the transports of carbon across 30°S for the globe, the Atlantic, the Indian, and the Pacific. The superimposed dark gray bars represent carbon transport estimates calculated using finer layer definitions. There are some subtle differences in the finer layer transports, but the agreement is remarkable.

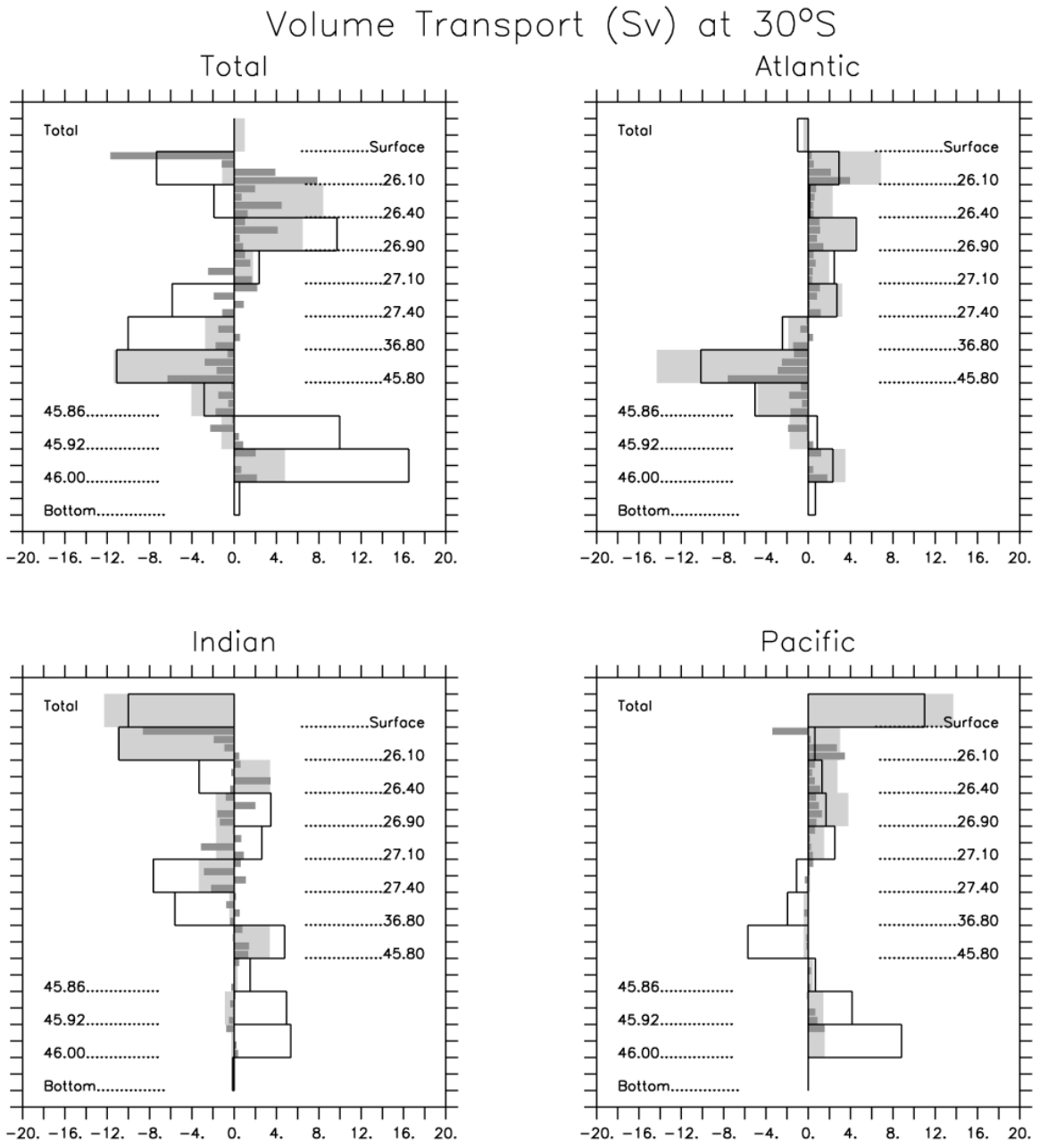

Figure 2. Inverse volume transports from the GFDL CM2.1 global climate model for the globally integrated transect at 30°S and for each ocean basin at 30°S. Black outlines delineate data-based inverse transport estimates; light gray bars are transports within these the defined data-based layers; dark gray bars subdivide each layer into four sublayers for improved vertical resolution. Positive values indicate northward transport (Sv).

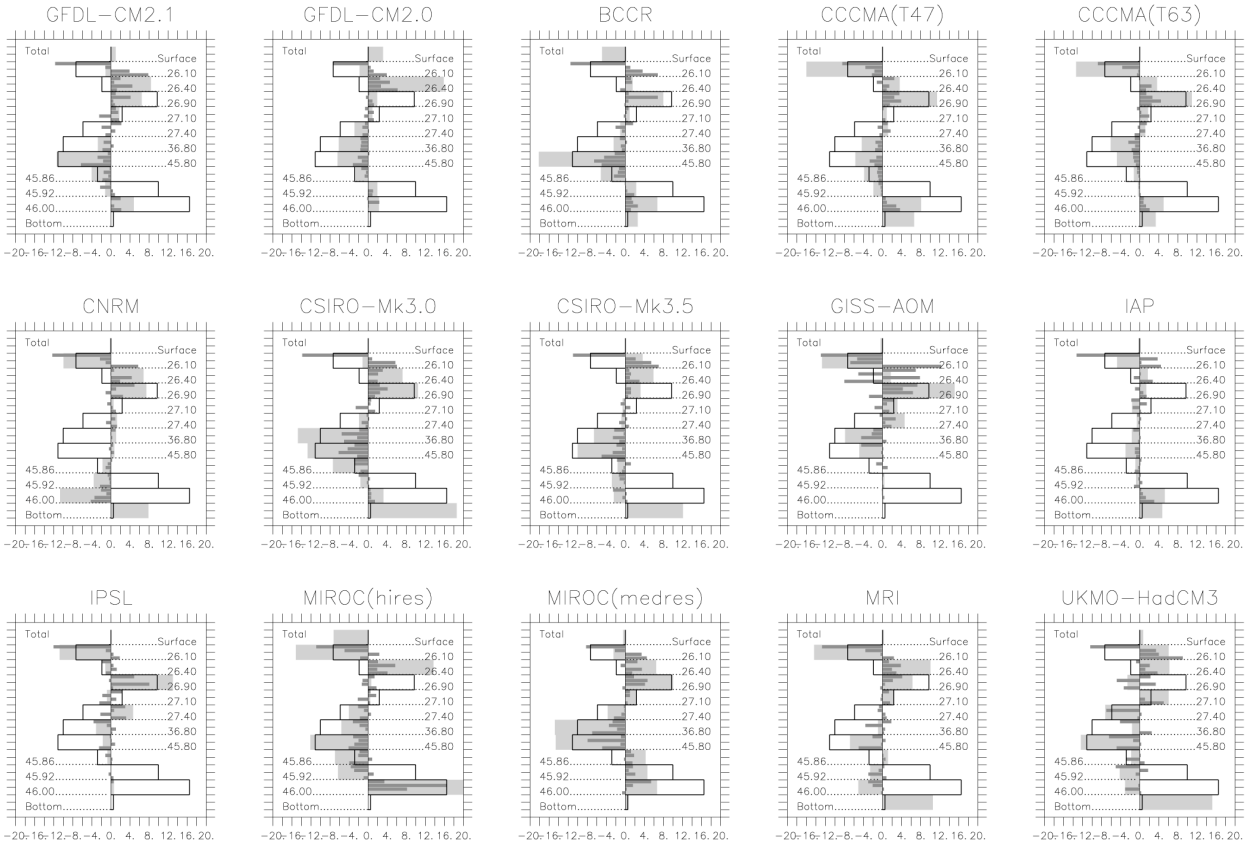

Figure 3.
Volume transports for each member of the model ensemble, as in Figure 2.

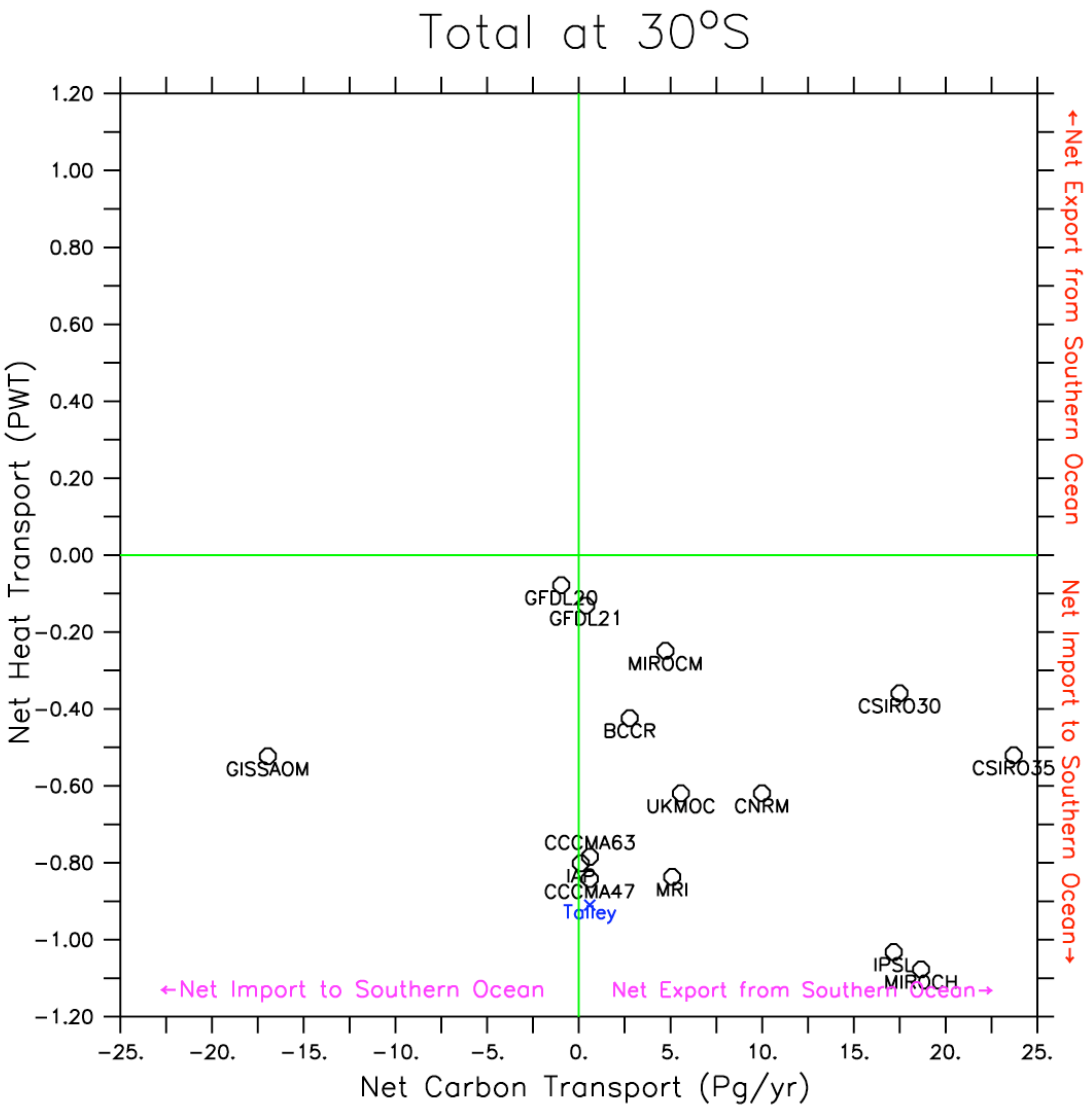

Figure 4. Model ensemble net heat and carbon transports across 30°S. The blue "x" plots observation-based estimates [*Talley,* 2008].